Horizontal Transition of Turbulent Cascade in the Near-Surface Layer of Tropical Cyclones

JIE TANG

Shanghai Typhoon Institute, China Meteorological Administration, Shanghai, and Key Laboratory of Mesoscale Severe Weather, Ministry of Education, and School of Atmospheric Sciences, Nanjing University, Nanjing, China

DAVID BYRNE

Environmental Physics Group, Institute of Biogeochemistry and Pollutant Dynamics, ETH Zürich, Zurich, Switzerland

JUN A. ZHANG

National Oceanic and Atmospheric Administration/Atlantic Oceanographic and Meteorological Laboratory/Hurricane Research Division, Miami, Florida

YUAN WANG

Key Laboratory of Mesoscale Severe Weather, Ministry of Education, and School of Atmospheric Sciences, Nanjing University, Nanjing, China

XIAO-TU LEI, DAN WU, PING-ZHI FANG, AND BING-KE ZHAO

Shanghai Typhoon Institute, China Meteorological Administration, Shanghai, China

(Manuscript received 15 December 2014, in final form 7 July 2015)

ABSTRACT

Tropical cyclones (TC) consist of a large range of interacting scales from hundreds of kilometers to a few meters. The energy transportation among these different scales—that is, from smaller to larger scales (upscale) or vice versa (downscale)—may have profound impacts on TC energy dynamics as a result of the associated changes in available energy sources and sinks. From multilayer tower measurements in the low-level (<120 m) boundary layer of several landing TCs, the authors found there are two distinct regions where the energy flux changes from upscale to downscale as a function of distance to the storm center. The boundary between these two regions is approximately 1.5 times the radius of maximum wind. Two-dimensional turbulence (upscale cascade) occurs more typically at regions close to the inner-core region of TCs, while 3D turbulence (downscale cascade) mostly occurs at the outer-core region in the surface layer.

1. Introduction

Tropical cyclones (TC) consist of a large range of interacting scales from hundreds of kilometers to a few meters. A change in how energy is transferred among these scales—that is, from smaller to larger scales (upscale) or vice versa (downscale)—can have profound impacts on TC energy dynamics as a result of the associated changes in available energy sources and sinks. This is because TC intensity is controlled by physical processes with different scales that are both external and internal to the storm (e.g., Marks and Shay 1998; Rogers et al. 2013). The external processes are associated with the large-scale flow surrounding the hurricane (e.g., Kaplan et al. 2010; Riemer et al. 2010; Tang and Emanuel 2012; Molinari et al. 2013). On the other hand, the internal processes are relatively small-scale processes (e.g., vortex scale, convective scale, turbulent scale) occurring within the hurricane (e.g., Emanuel 1995; Nolan et al. 2007; Vigh and Schubert 2009; Cione et al. 2013; Montgomery et al. 2014; Rogers et al. 2015).

Corresponding author address: Prof. Yuan Wang, School of Atmospheric Sciences, Nanjing University, No. 22 Hankou Road, Nanjing, Jiangsu 210093, China.
E-mail: yuanasm@nju.edu.cn

DOI: 10.1175/JAS-D-14-0373.1

One key advance in our knowledge of tropical cyclone dynamics is that turbulent processes in the boundary layer are a key mechanism for the development and maintenance of tropical cyclones (Emanuel 1986, 1991; Emanuel et al. 1987; Bryan and Rotunno 2009; Smith et al. 2009). However, despite these developments, dynamical models, which are based upon our current knowledge, are typically outperformed by purely statistical models when predicting storm intensity and rapid intensification (RI) (Kaplan et al. 2010; Gall et al. 2013). While there may be many causes for this, one potential reason is that we have failed to account for a key aspect of turbulence, that under certain flow constraints, the energy dynamics of the entire system can fundamentally change; that is, energy can be transferred from smaller to larger scales (Kraichnan 1967) or vice versa (Kolmogorov 1941). Depending on which regime is active, this energy cascade process can have profound impacts on the tropical cyclone's available energy sources and sinks. This change in energy dynamics depends upon the dimensionality of turbulence, whether it is 2D (upscale energy transfer) or 3D (downscale energy transfer). Furthermore, typically 2D turbulence exists when the flow is restricted via some external means to only flow in a single plane (i.e., 3D motions are strongly suppressed)—for example, geometric confinement (Xia et al. 2009, 2008), vertical shear, stratification, and/or rotation (De Verdiere 1980).

While a single, or indeed multiple constraints may be active at any one time and lead to a 2D turbulence regime, these conditions can of course be broken and the flow can return to a 3D turbulence state where energy once again flows downscale. A further complication is that recently it has been shown that 2D and 3D turbulence can even coexist (Smith et al. 1996; Celani et al. 2010). While laboratory and direct numerical simulations have made significant advances for when these differing constraints for 2D break down (Smith et al. 1996; Celani et al. 2010; Hopfinger et al. 1982; Xia et al. 2011; Byrne et al. 2011), such knowledge has never been applied in the context of TCs. It is clear that tropical cyclones offer conditions for 2D turbulence; however, when, how, and to what extent remain largely uninvestigated.

Direct measurement of turbulent properties is very difficult to achieve given the severe condition in TCs (Zhang et al. 2011; Zhang and Montgomery 2012); thus, few studies have investigated the energy cascade in the TCs. Zhu et al. (2010, hereafter Z10) analyzed 10-m surface wind data of several landfall hurricanes and found that there exists 3D direct energy cascade in tropical cyclone boundary layer (TCBL), which is similar with the elevator-like concept model (Hunt and Carlotti 2001, hereafter HC01) (see Fig. 6 in Z10 and Fig. 10 in HC01). Byrne and Zhang (2013, hereafter BZ13) found via aircraft in situ data collected during the Coupled Boundary Layer Air–Sea Transfer (CBLAST) experiment (Black et al. 2007; Zhang et al. 2008; Zhang and Drennan 2012) that both 2D and 3D turbulence exist in the TCBL. BZ13 also found there was a height-dependent transition of turbulent flow regime from 3D to 2D turbulence where the inverse energy cascade occurs above ~150 m while direct energy cascade occurs below 150 m above the sea surface. While these initial investigations provide compelling evidence that there are changes in the energy dynamics of the flow within the TCBL, there still remain many unanswered questions. BZ13 note that, because of safety constraints, the aircraft data used for the analysis were mainly collected between hurricane rainbands where it is still far from the hurricane center and under conditions of weak convection. How the turbulence energy dynamics change in the other areas of the TCBL, where conditions for 2D could be broken (i.e., via strong convection, especially in the inner-core region) remains poorly understood.

Here we aim to bridge this gap. This paper investigates the energy cascade process in the near-surface layer during the landfall of three typhoons in 2010 and analyzes the high-frequency wind data collected by a high (~100 m) offshore tower equipped with anemometers at different altitudes. The tower data allow us to explore the variability of turbulence energy cascade process under different locations relative to the storm center and different convective environments.

2. Data and analysis method

The data used in this study was collected by a near-surface multilayer onshore tower located at Zhangpu of Fujian province of China (24.04°N, 117.90°E). This tower collected data from three landfall typhoons in 2010 [Tropical Storm Lionrock (1006), Typhoon Fanapi (1011), and Typhoon Megi (1015)] as shown in Fig. 1. Typhoon tracks with 6-h interval are from China Meteorology Administration (CMA) best track (Fig. 1). Distances from the tower to the typhoon center are based on China Meteorology Administration operation track with 1-h interval and are also shown in Table 1. The period of interest covers the whole landfall stage of these three typhoons from 8 h before landfall to the time of landfall. The 3D wind velocity was measured via four WindMaster Pro three-dimensional supersonic anemometers produced by British Gill at different altitudes (56, 72, 89, and 111 m) on the tower, with wind data sampled at 20 Hz. The radius maximum wind (RMW) showed in Table 1 are estimated at a height of 1 km from

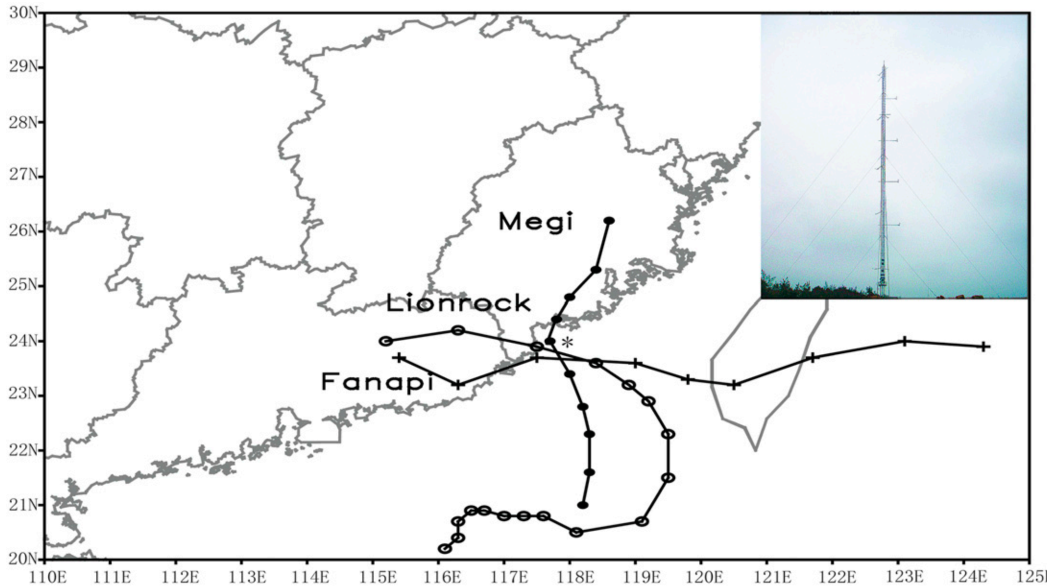

FIG. 1. Tracks of Typhoons Lionrock, Fanapi, and Megi (2010). The location of the Zhangpu tower is denoted by the asterisk just off the coast near where the three trajectories intersect. A photo of the tower is shown at the upper right of the figure.

Xiamen radar (located at 24.05°N, 118.08°E and 185.1 m in altitude) and based on ground-based velocity track display (GBVTD) technique (Zhao et al. 2008).

The frozen turbulence assumption is used to convert time series data to spatial variations following BZ13, which is typically valid if the fluctuation of wind V' is smaller than 10% of the mean wind $\overline{V}$ (here taken as the 10-min running mean). Indeed, this condition is satisfied with the turbulence intensity (Frisch 1995)

$$I = \frac{\sqrt{\langle V'^2 \rangle}}{\overline{V}} \ll 1, \tag{1}$$

where the angle brackets denote an ensemble average.

Figure 2 shows an example of the wind variation and its kinetic energy spectrum computed from the converted time series data to a measure of spatial variation under the Taylor frozen turbulence assumption for Typhoon Megi at 111 m during the landfall. During the period (Fig. 2a), the wind speed stayed steady with an average value of $\sim 30\,\mathrm{m\,s^{-1}}$ and fluctuations in the range from 25 to $35\,\mathrm{m\,s^{-1}}$. The frequency distribution of the turbulence intensity for this leg is shown in Fig. 2c. It is evident for the figure that the majority (>75%) of the data have turbulence intensity (<0.05), which satisfies the requirement for turbulence frozen assumption according to Eq. (1). The variation of the wind direction of this leg also remains nearly steady (Fig. 2d). Following this quality-control procedure, we selected 1-h data for each observation leg. That is to say, there are 72 000 observation samples for every observation leg. There are a total of nine legs for each observation height (56, 72, 89, and 111 m) in each typhoon (Table 1). The observational legs that did not pass the quality-control procedure are defined as data absence and discarded in this study (e.g., −3 h of Fanapi, −2 and −3 h of Lionrock, and −7 h of Megi in Table 1).

The wind spectrum shows energy distributed among a broadband of scales from the order of 10^1 to 10^6 m (Fig. 2b). While the spectral signal is noisy, there is an indication that there exists an inertial range consistent with a turbulent flow—that is, in agreement with Kolmogorov–Kraichnan $K^{-5/3}$ scaling law (blue dotted line)—from the 10^1-m scale to 10^3 m. In the range from 10^3 to 10^4 m, the spectral slope steepens. At larger scale (>10^4 m), the spectral slope levels off. In terms of the dominant energy containing scales, both 2D and 3D turbulence theory predict the same $K^{-5/3}$ law. Thus it is not possible to determine whether the turbulent flux is a direct (3D) cascade or inverse (2D) energy cascade. Note that the wind spectrum collected in other prelandfall period and other height of the three typhoons showed a similar behavior as the example shown above.

To clarify the direction of the energy cascade, we compute the two-point horizontal velocity difference $\delta v_u = \langle (v_{x+L} - v_x)^n \rangle$ of the velocity component parallel to L for each observation height and v_x is the wind velocity at the position x following BZ13. The third

TABLE 1. Summary of the analysis result for all the legs at a height of 111 m in Typhoons Fanapi, Lionrock, and Megi, including the energy flux, distance to Zhangpu tower, and the intensity of the typhoons in their landing stage.

	Fanapi					Lionrock					Megi				
Hours before landing	Distance (km)	RMW (km)	1-h mean wind ($m\,s^{-1}$)	Average energy flux ($10^{-5}\,m^2\,s^{-3}$)	TKE production ($10^{-5}\,m^2\,s^{-3}$)	Distance (km)	RMW (km)	1-h mean wind[a] ($m\,s^{-1}$)	Average energy flux ($10^{-5}\,m^2\,s^{-3}$)	TKE production ($10^{-5}\,m^2\,s^{-3}$)	Distance (km)	RMW (km)	1-h mean wind ($m\,s^{-1}$)	Average energy flux ($10^{-5}\,m^2\,s^{-3}$)	TKE production ($10^{-5}\,m^2\,s^{-3}$)
−8	179.2	75	13.7	**58.5**[b]	65.8	127.9	30	10.1	**0.2**	8.8	105.3	25	24.3	**29.8**	109.0
−7	164.9	75	14.4	*−3.3*	42.3	112.4	30	10.5	**3.0**	96.8	92.6	45	25.2	NaN	15.0
−6	140.4	70	15.6	**61.7**	135.3	88.5	37	12.0	**16.0**	211.7	81.7	45	26.6	**148.3**	222.3
−5	130.2	70	17.8	**16.0**	52.0	73.0	45	13.8	**13.4**	36.3	70.8	33	27.5	**32.9**	112.6
−4	116.0	67	18.0	**29.5**	144.1	65.1	45	13.1	**11.5**	26.7	59.0	45	28.2	**2.3**	153.3
−3	89.3	65	18.7	NaN	NaN	52.8	44	17.0	NaN[c]	NaN	48.0	45	28.3	*−47.5*	141.5
−2	66.1	57	16.6	*−98.4*	139.6	38.6	45	21.8	NaN	NaN	38.6	45	28.5	*−84.8*	93.0
−1	34.0	40	16.8	*−19.6*	82.7	28.2	41	23.3	−91.5	141.8	28.2	42	28.7	*−153*	161.7
0	42.0	45	20.8	*−89.9*	149.8	42.0	37	24.6	−112.8	441.1	26.6	43	30.0	*−1.1*	27.8
Average percentage of energy flux to TKE production[d]					41.5%[d]					26.2%					43.5%

[a] The 1-h position of three typhoons came from CMA operation track.
[b] Boldface numbers denote positive energy flux ϵ (3D direct cascade); italic numbers denote negative energy flux ϵ (2D inverse cascade).
[c] NaN indicates that the data for this period are absent or nonqualified for the calculation of the structure function.
[d] This average percentage from 0 to −8 h of energy flux to TKE production.

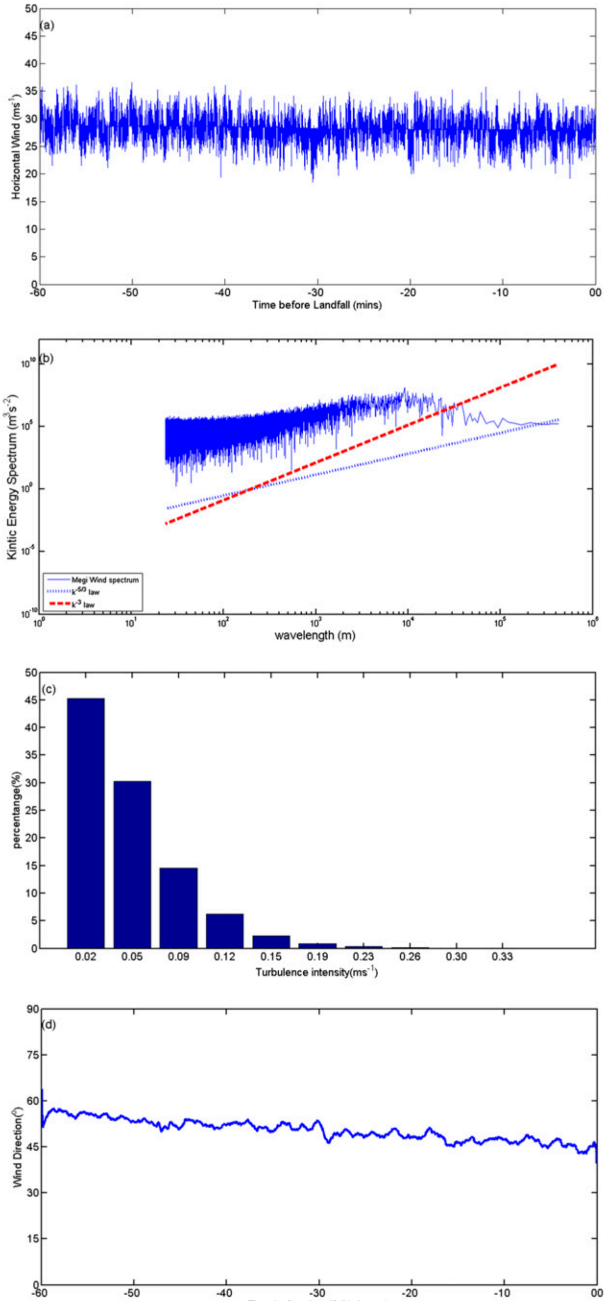

FIG. 2. Data from a typical leg for energy flux calculations. Plots of (a) horizontal wind speed vs time before landfall, (b) kinetic energy spectrum, (c) frequency distribution of turbulence intensity, and (d) 1-min-averaged horizontal wind direction before landfall.

moment $S_{3L} = \delta v_u^3$ gives the value and the direction of the energy flux ϵ across the scale L (Frisch 1995):

$$\epsilon = -\frac{2}{3}S_{3L}/L. \tag{2}$$

Therefore, the sign of S_{3L} indicates the direction of the energy flux, where a positive S_{3L} (negative ε) signifies an inverse cascade and a negative S_{3L} (positive ε) a downward cascade (Xia et al. 2011).

3. Results

Data analysis results for all the observation legs are summarized in Table 1. Figures 3, 4, and 5 show the third-order structure function (S_{3L}) as a function of scale L for Typhoons Fanapi, Lionrock, and Megi, respectively, at four levels. In general, S_{3L} is a quasi-linear function of L for all the legs, in agreement with Eq. (2). In all three typhoons, S_{3L} tends to change from negative to positive values as the storm is approaching land. When the typhoon is far from the tower (<4 h before landfall), S_{3L} is either close to zero (e.g., Fig. 5) or negative (e.g., Fig. 4). As the typhoon moves closer to the tower (<4 h before landfall), S_{3L} became positive with increasing values.

It is evident from Figs. 3–5 that the inverse cascade (i.e., positive S_{3L}) occurs at all the measurement heights in all three typhoons. However, comparing S_{3L} at different heights in each typhoon, there is no apparent transition between different heights. Plotting the energy flux as a function of height for all the legs (Fig. 6) confirms that there is no height-dependent transition from 3D to 2D cascade in our analyses. This result is somewhat different from that of BZ13, who found that there is a vertical transition of turbulent energy cascade from 3D to 2D. However, our measurements taken from a fixed tower are all below 150 m, which is the threshold found by BZ13 for the height-dependent transition. Furthermore, the measurements of BZ13 were taken at the outer-core region (>100 km from the storm center) over the open ocean. It will be shown later (cf. Fig. 11) that when our data are grouped as a function of distance to the storm center, most of the legs in the outer-core region show 3D energy cascade (i.e., positive energy flux), which is consistent with BZ13 given the measurement heights are below 150 m.

It is evident from Fig. 6 that a number of legs have values of energy flux close to zero. These legs correspond to those shown in Figs. 3–5, where S_{3L} is also close to zero (e.g., −5 h of Fanapi in Fig. 3, −7 h of Lionrock in Fig. 4, and −6 h of Megi in Fig. 5). To understand the detail of energy flux, Figs. 7–9 show the energy flux as a function of L for Typhoons Fanapi, Lionrock, and Megi, respectively, for all the legs at 111-m height. It appears that the energy flux has the same sign for the entire range of L for most (>80%) legs. And Figs. 7–9 showed a more remarkable cascade transition from positive energy flux (3D energy cascade) to negative energy flux (2D energy cascade) than Figs. 3–5 when typhoons move closer and closer. Interestingly, it is

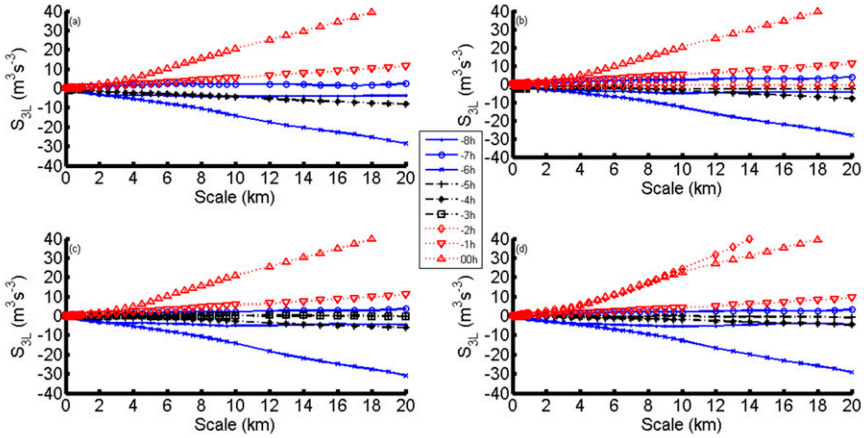

FIG. 3. Plot of the structure function S_{3L} as a function of scale in Typhoon Fanapi (2010) at heights (a) 56, (b) 72, (c) 89, and (d) 111 m. Different types and colors of lines represent different hours before typhoon landfall as shown in the legend with the blue lines indicating −8, −7, and −6 h; the black lines indicating −5, −4, and −3 h; and the red lines indicating −2, −1, and 0 h.

found in some legs in Typhoon Fanapi that turbulence transition from positive energy flux (direct 3D turbulence cascade) to negative ϵ (inverse 2D turbulence cascade) occurred at different scales (Fig. 7) or vice versa. For example, in the case of −6 h of Fanapi (Fig. 7), the smaller scales support an inverse cascade and the larger scales a direct cascade. This maybe implies a dual cascade with two energy sources. One for the 2D flux, potentially coming from small-scale convective processes or shear generation and the other direct cascade coming from the parent vortex; that is, one cascade (2D or 3D) does not dominate and the energy flux is still transient in some region of TCBL.

Figure 10 shows the energy flux as a function of wind speed averaged for each leg at 111 m. Although the energy flux can be either positive or negative at a given wind speed, the majority (>70%) of the legs with wind speed > 20 m s^{-1} have negative values. Vice versa, the majority (>75%) of the legs with wind speed < 20 m s^{-1} have positive values. This result indicates that 2D energy cases tends to happen in the surface layer (≤111 m) in high wind conditions.

The energy flux is plotted as a function of radius to the storm center normalized by the radius of maximum wind speed (RWM) in Fig. 11. A clear separation of positive and negative values of the energy flux is seen at r/RMW ~ 1.5. This result indicates that there is a transition from 3D to 2D turbulent cascade depending on the location of the storm relative to the eyewall region (i.e., RMW). This finding is robust for all three typhoons,

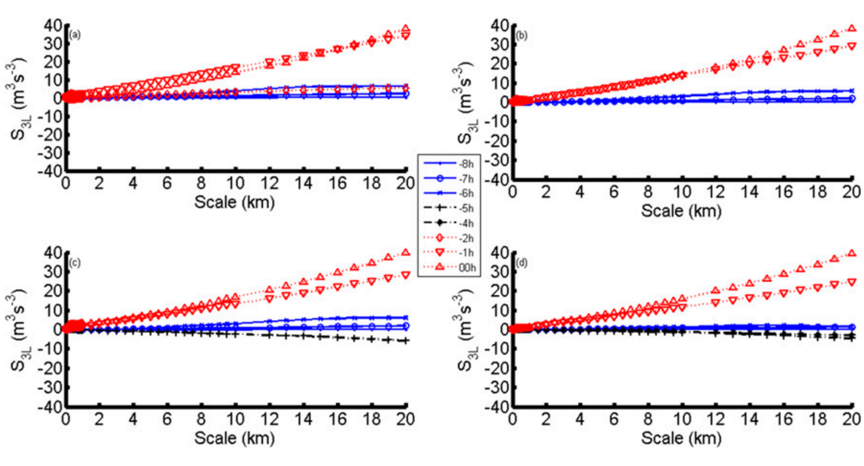

FIG. 4. As in Fig. 3, but for Typhoon Lionrock (2010) and without the black line representing −3 h.

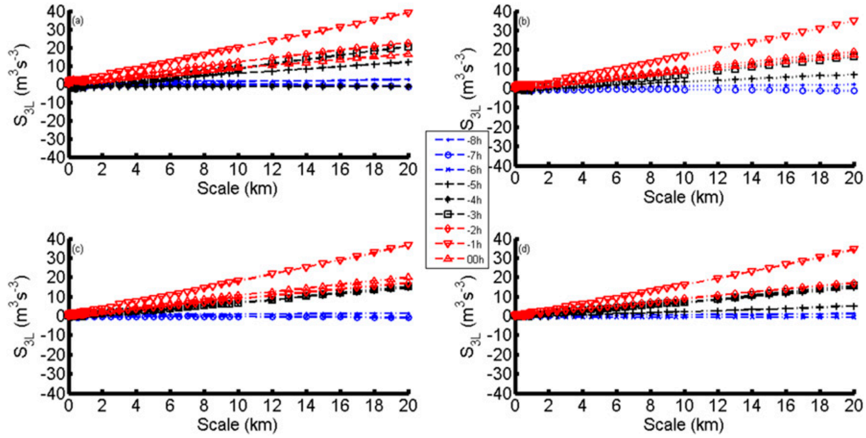

FIG. 5. As in Fig. 3, but for Typhoon Megi (2010).

showing that 3D direct turbulence cascade and turbulent energy dissipation is preferred in the outer region while 2D inverse turbulence cascade and turbulent energy accumulation is dominant in the inner core. As mentioned earlier, this result is consistent with BZ13 in that 3D turbulence cascade is found in the outer region of TCs below 150 m.

To verify the relative contribution of cascade transportation, the production of turbulent kinetic energy $[\mathrm{TKE} = (1/2)(u'^2 + v'^2 + w'^2)^{1/2}]$ is calculated (Table 1). At 111 m, the computed 1-h-averaged TKE production varies from 8.8×10^{-5} to $441.1 \times 10^{-5}\,\mathrm{m^2\,s^{-3}}$ during the landing stage of the three typhoons. The average energy flux ε is approximately 26.2%, 41.5%, and 43.5% of the total TKE production for Typhoon Lionrock, Fanapi, and Megi, respectively, as shown by Table 1. This considerable portion of cascade energy flux in the total TKE variation shows that the direct and inverse cascades are quite important to the turbulent process.

4. Discussion and conclusions

In this study, we investigate turbulent energy cascade processes in the near-surface layer of landfall typhoons using anemometer measured wind data from a multilayer high tower with a maximum height of 111 m above the sea surface. We found there is a horizontal transition between 2D turbulence (negative cascade) and 3D turbulence (direct cascade) for turbulent flow below 111 m at locations near a distance of 1.5 times the RMW. With

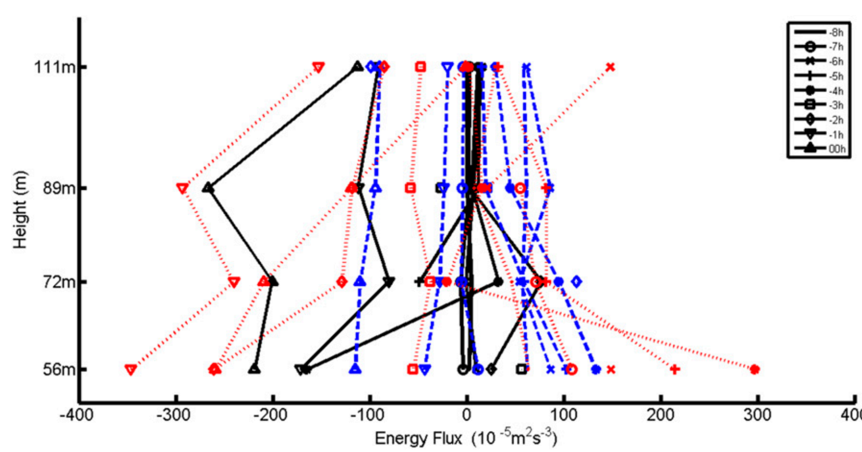

FIG. 6. Plot of energy flux (ϵ) as a function of height for all the legs in the three typhoons. Blue dashed lines represent Typhoon Fanapi, black solid lines represent Typhoon Lionrock, and red dotted lines represent Typhoon Megi. Lines with or without different symbols represent different hours before landfall: −8 (no symbols), −7 (open circles), −6 (× symbols), −5 (short vertical lines), −4 (filled circles), −3 (open squares), −2 (diamonds), −1 (downward triangles), and 0 (regular triangles).

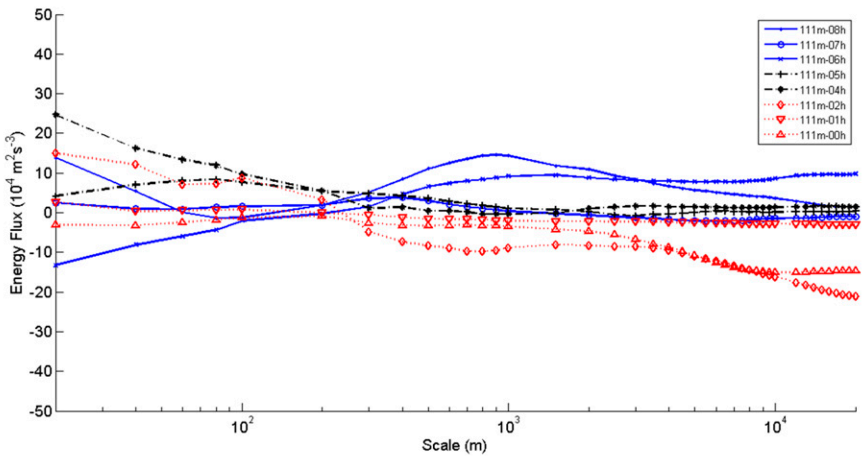

FIG. 7. Plot of the energy flux (ϵ) as a function of scale (L) at a height of 111 m during the landfall period of Typhoon Fanapi. Different types and colors of lines represent different hours before typhoon landfall as shown in the legend with the blue lines indicating −8, −7, and −6 h; the black lines indicating −5, and −4, h; and the red lines indicating −2, −1, and 0 h.

2D turbulence (and turbulent energy accumulation) active in the inner core (i.e., <1.5 RMW) and 3D turbulence (and turbulent energy dissipation) in the outer-core region (i.e., >1.5 RMW).

Our results, combined with those of BZ13, potentially provide a different perspective with which to understand TC dynamics. Recasting the problem in terms of the spectral energy flux, (i.e., the transfer of energy among different scales) can be a powerful tool and may reveal processes not considered before.

The characteristic that sets a turbulent flow apart from a laminar or chaotic flow is the existence of the energy cascade, such that, in the classical 3D picture, from a defined forcing scale L energy cascades at some constant rate η to the scale where it is dissipated. The case is likely far more complicated for tropical cyclones where there exist multiple forcing scales; however, here we will broadly categorize them to two forcing scales. First, large-scale forcing ($L > 100$ km), which arises from large-scale temperature–pressure gradients, which because of its relative horizontal scale compared to the depth of the atmosphere is essentially 2D forcing. Second, there also exists small-scale 3D forcing (~km) due to convective processes. The question arises then as where the intermediate scales between get their energy and more importantly, in such a system, how is energy dissipated?

Indeed, the first question has been addressed in turbulence laboratory experiments in fluid layers, where a large-scale vortex, whose horizontal scale was much larger than the fluid thickness, was forced over the top of an underlying small-scale 3D forcing. It was shown that the large-scale vortex enforces 2D and induces an

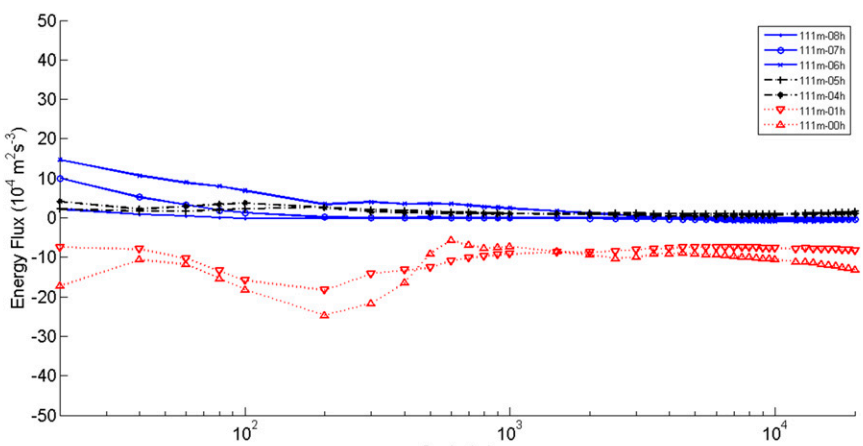

FIG. 8. As in Fig. 7, but for Typhoon Lionrock and without the red line representing −2 h.

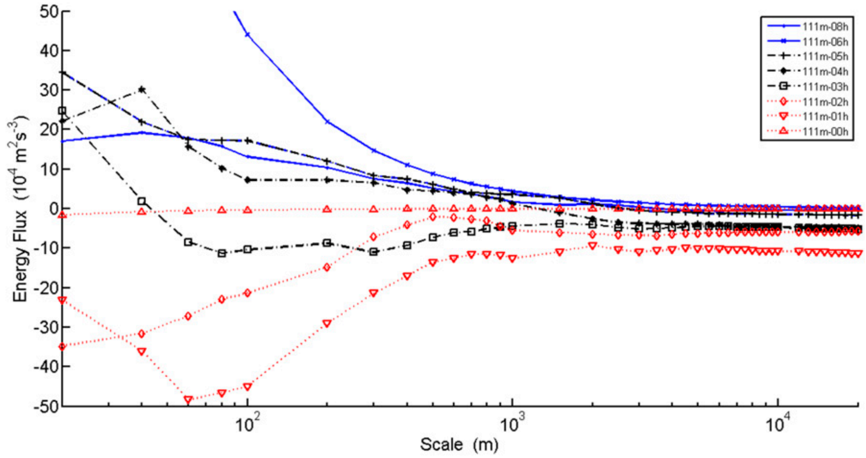

FIG. 9. As in Fig. 7, but for Typhoon Megi and without the blue line representing −7 h and with an additional black line representing −3 h.

upscale energy flux through the intermediate scales (Xia et al. 2011).

This of course leads to very strong implications for energy dissipation in the system. For tropical cyclones, there are two dissipative mechanisms for momentum available, which one can represent via external friction and the other via the 3D cascade to the viscous scale. First, the presence of external friction is a linear dissipation that affects all scale sizes equally, which, in a quasi-2D flow, is typically parameterized via Rayleigh friction $\alpha_{2D} = \nu\pi^2/2h^2$ with ν being viscosity and h the layer depth. The addition of 3D motions increases dissipation in the system above its lower 2D limit and may be represented by an ''eddy viscosity'' term K, where 3D eddies more efficiently transport momentum from the higher layers to the surface; that is, $\alpha_{3D} = (\nu + K)\pi^2/2h^2$ (Shats et al. 2010). The quantity K is typically much higher if a 3D energy cascade is also supported and energy can be dissipated at the viscous scale internally. Therefore, as two-dimensional constraints begin to be imposed on the system, then K begins to reduce until one reaches the lower 2D friction limit. Of particular interest is that the dissipation in the system determines the largest-scale size that can be supported for a given energy injection.

This poses the question as to whether the insights gained from focused turbulence laboratory experiments can be applied to tropical cyclones. In the context of the results presented here and BZ13, we would argue that such insights may be widely applicable. Within this framework we propose the following. During TC genesis, the large-scale parent vortex and the small convective forcing scales are disparate. After some time, the parent vortex starts to impose two-dimensional

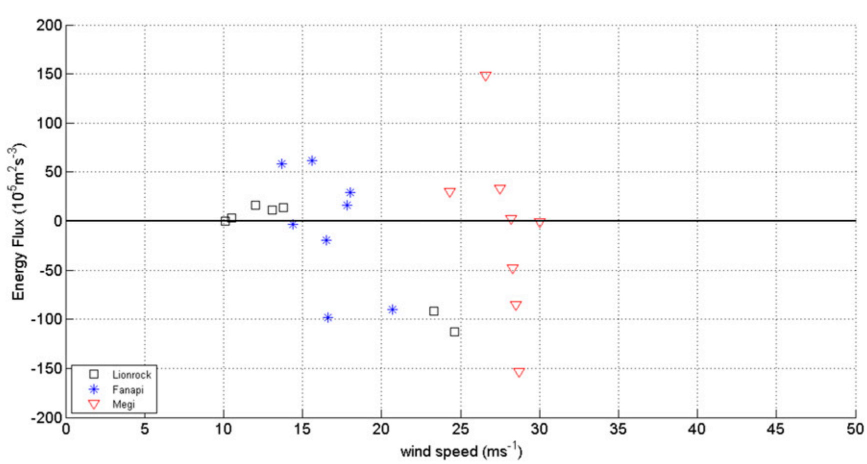

FIG. 10. Plot of energy flux as a function of wind speed with blue asterisks for Fanapi, black squares for Lionrock, and red downward triangles for Megi.

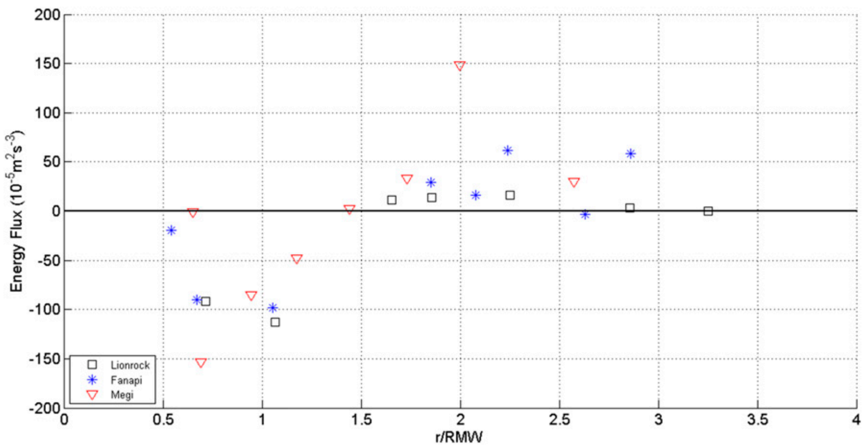

FIG. 11. Plot of the energy flux as a function of radius normalized by RMW with symbols as in Fig. 10.

constraints to the underlying 3D forcing. This begins to reduce dissipation, which allows for energy to be from smaller scales to larger scales and larger scales, which in turn strengthens two dimensionalities and reduces dissipation further. This cycle therefore may connect the large-scale parent vortex with the induced upscale energy flux, essentially securing a new energy source that should be included in the maximum potential intensity. Alternatively, there may be some instances where the two-dimensional constraints are not dominant and therefore dissipation is not reduced sufficiently for energy to reach the parent vortex (i.e., 3D dominates). In such a case, then, only the large-scale forcing can sustain the parent vortex, or the parent vortex must shrink in size to that determined by the dissipation in the system. This indeed could be the reason for the differing 2D and 3D regions as a function of radius.

This picture may also offer a new explanation for the observed reduction in sea drag. Currently, all theories to explain the effect are related to wind–wave interaction or controlled by bottom-up processes. Here we offer that this may be explained via a top-down process, where the large-scale parent vortex imposes two dimensionalities on the underlying flow and, by suppressing the 3D turbulent flux, reduces the vertical flux of momentum to the boundary and, as such, leads to the reduction in sea drag (e.g., Powell et al. 2003; Black et al. 2007; French et al. 2007).

While our study is based on a single tower observation for several TC cases, the result adds to the mounting evidence that the large-scale parent vortex of TCs may gain energy directly from small scales. As highlighted above, the implications for the energy dynamics of TCs are very important and, as such, we may need to reconsider how we represent such effects in the turbulence schemes of dynamical models. This paper, combined with BZ13, are only small steps to reach such a goal; however, they provide the motivation for a comprehensive field experiment with simultaneous airborne and ground-based instruments in the TCBL that would be required to fully understand the turbulent transport processes and their role on TC intensity change.

Acknowledgments. This work is supported by the Major State Basic Research Development Program of China (2015CB452801 and 2013CB430305), the National Natural Science Foundation of China (41475060 and 41275057), and the Public Benefit Research Foundation of China (GYHY201406010). Jun Zhang was supported by NOAA's Hurricane Forecast and Improvement Project (HFIP) Grant NA14NWS4680028 and NASA Grant NNX14AM69G. David Byrne was supported by ETH Research Grant CH2-01-11-1. We also thank three reviewers for their comments that helped substantially improve our paper.

REFERENCES

Black, P. G., and Coauthors, 2007: Air–sea exchange in hurricanes: Synthesis of observations from the Coupled Boundary Layer Air–Sea Transfer experiment. *Bull. Amer. Meteor. Soc.*, **88**, 357–374, doi:10.1175/BAMS-88-3-357.

Bryan, G. H., and R. Rotunno, 2009: The maximum intensity of tropical cyclones in axisymmetry numerical model simulations. *Mon. Wea. Rev.*, **137**, 1770–1789, doi:10.1175/2008MWR2709.1.

Byrne, D., and J. A. Zhang, 2013: Height-dependent transition from 3-D to 2-D turbulence in the hurricane boundary layer. *Geophys. Res. Lett.*, **40**, 1439–1442, doi:10.1002/grl.50335.

——, H. Xia, and M. Shats, 2011: Robust inverse energy cascade and turbulence structure in three-dimensional layers of fluid. *Phys. Fluids*, **23**, 095109, doi:10.1063/1.3638620.

Celani, A., S. Musacchio, and D. Vincenzi, 2010: Turbulence in more than two and less than three dimensions. *Phys. Rev. Lett.*, **104**, 184506, doi:10.1103/PhysRevLett.104.184506.

Cione, J. J., E. A. Kalina, J. A. Zhang, and E. W. Uhlhorn, 2013: Observations of air–sea interaction and intensity change in hurricanes. *Mon. Wea. Rev.*, **141**, 2368–2382, doi:10.1175/MWR-D-12-00070.1.

De Verdiere, A. C., 1980: Quasi-geostrophic turbulence in a rotating homogeneous fluid. *Geophys. Astrophys. Fluid Dyn.*, **15**, 213–251, doi:10.1080/03091928008241179.

Emanuel, K. A., 1986: An air-sea interaction theory for tropical cyclones. Part I: Steady-state maintenance. *J. Atmos. Sci.*, **43**, 585–605, doi:10.1175/1520-0469(1986)043<0585:AASITF>2.0.CO;2.

——, 1991: The theory of hurricanes. *Annu. Rev. Fluid Mech.*, **23**, 179–196, doi:10.1146/annurev.fl.23.010191.001143.

——, 1995: Sensitivity of tropical cyclones to surface exchange coefficients and a revised steady-state model incorporating eye dynamics. *J. Atmos. Sci.*, **52**, 3969–3976, doi:10.1175/1520-0469(1995)052<3969:SOTCTS>2.0.CO;2.

——, M. Fantini, and A. J. Thorpe, 1987: Baroclinic instability in an environment of small stability to slantwise moist convection. Part I: Two-dimensional models. *J. Atmos. Sci.*, **44**, 1559–1573, doi:10.1175/1520-0469(1987)044<1559:BIIAEO>2.0.CO;2.

Frisch, U., 1995: *Turbulence: The Legacy of A. N. Kolmogorov*. Cambridge University Press, 312 pp.

French, J. R., W. D. Drennan, J. A. Zhang, and P. G. Black, 2007: Turbulent fluxes in the hurricane boundary layer. Part I: Momentum flux. *J. Atmos. Sci.*, **64**, 1089–1102, doi:10.1175/JAS3887.1.

Gall, R., J. Franklin, F. Marks, E. N. Rappaport, and F. Toepfer, 2013: The Hurricane Forecast Improvement Project. *Bull. Amer. Meteor. Soc.*, **94**, 329–343, doi:10.1175/BAMS-D-12-00071.1.

Hopfinger, E., F. K. Browand, and Y. Gagne, 1982: Turbulence and waves in a rotating tank. *J. Fluid Mech.*, **125**, 505–534, doi:10.1017/S0022112082003462.

Hunt, J. C. R., and P. Carlotti, 2001: Statistical structure at the wall of the high Reynolds number turbulent boundary layer. *Flow Turbul. Combust.*, **66**, 453–475, doi:10.1023/A:1013519021030.

Kaplan, J., M. DeMaria, and J. A. Knaff, 2010: A revised tropical cyclone rapid intensification index for the Atlantic and eastern North Pacific basins. *Wea. Forecasting*, **25**, 220–241, doi:10.1175/2009WAF2222280.1.

Kolmogorov, A. N., 1941: The local structure of turbulence in incompressible viscous fluid for very large Reynolds numbers. *Dokl. Akad. Nauk SSSR*, **30**, 301–305.

Kraichnan, R. H., 1967: Inertial ranges in two-dimensional turbulence. *Phys. Fluids*, **10**, 1417, doi:10.1063/1.1762301.

Marks, F. D., and L. K. Shay, 1998: Landfalling tropical cyclones: Forecast problems and associated research opportunities. *Bull. Amer. Meteor. Soc.*, **79**, 305–323.

Molinari, J., J. Frank, and D. Vollaro, 2013: Convective bursts, downdraft cooling, and boundary layer recovery in a sheared tropical storm. *Mon. Wea. Rev.*, **141**, 1048–1060, doi:10.1175/MWR-D-12-00135.1.

Montgomery, M. T., J. A. Zhang, and R. K. Smith, 2014: An analysis of the observed low-level structure of rapidly intensifying and mature hurricane *Earl* (2010). *Quart. J. Roy. Meteor. Soc.*, **140**, 2132–2146, doi:10.1002/qj.2283.

Nolan, D. S., Y. Moon, and D. P. Stern, 2007: Tropical cyclone intensification from asymmetric convection: Energetics and efficiency. *J. Atmos. Sci.*, **64**, 3377–3405, doi:10.1175/JAS3988.1.

Powell, M. D., P. J. Vickery, and T. A. Reinhold, 2003: Reduced drag coefficient for high wind speeds in tropical cyclones. *Nature*, **422**, 279–283, doi:10.1038/nature01481.

Riemer, M., M. T. Montgomery, and M. E. Nicholls, 2010: A new paradigm for intensity modification of tropical cyclones: Thermodynamic impact of vertical wind shear on the inflow layer. *Atmos. Chem. Phys.*, **10**, 3163–3188, doi:10.5194/acp-10-3163-2010.

Rogers, R., and Coauthors, 2013: NOAA's Hurricane Intensity Forecasting Experiment: A progress report. *Bull. Amer. Meteor. Soc.*, **94**, 859–882, doi:10.1175/BAMS-D-12-00089.1.

——, P. D. Reasor, and J. A. Zhang, 2015: Multiscale structure and evolution of Hurricane Earl (2010) during rapid intensification. *Mon. Wea. Rev.*, **143**, 536–562, doi:10.1175/MWR-D-14-00175.1.

Shats, M., D. Byrne, and H. Xia, 2010: Turbulence decay rate as a measure of flow dimensionality. *Phys. Rev. Lett.*, **105**, 264501, doi:10.1103/PhysRevLett.105.264501.

Smith, L. M., J. R. Chasnov, and F. Waleffe, 1996: Crossover from two-to three-dimensional turbulence. *Phys. Rev. Lett.*, **77**, 2467, doi:10.1103/PhysRevLett.77.2467.

Smith, R. K., M. T. Montgomery, and N. Van Sang, 2009: Tropical cyclone spin-up revisited. *Quart. J. Roy. Meteor. Soc.*, **135**, 1321–1335, doi:10.1002/qj.428.

Tang, B., and K. Emanuel, 2012: A ventilation index for tropical cyclones. *Bull. Amer. Meteor. Soc.*, **93**, 1901–1912, doi:10.1175/BAMS-D-11-00165.1.

Vigh, J. L., and W. H. Schubert, 2009: Rapid development of the tropical cyclone warm core. *J. Atmos. Sci.*, **66**, 3335–3350, doi:10.1175/2009JAS3092.1.

Xia, H., H. Punzmann, G. Falkovich, and M. Shats, 2008: Turbulence-condensate interaction in two dimensions. *Phys. Rev. Lett.*, **101**, 194504, doi:10.1103/PhysRevLett.101.194504.

——, M. Shats, and G. Falkovich, 2009: Spectrally condensed turbulence in thin layers. *Phys. Fluids*, **21**, 125101, doi:10.1063/1.3275861.

——, D. Byrne, G. Falkovich, and M. Shats, 2011: Upscale energy transfer in thick turbulent fluid layers. *Nat. Phys.*, **7**, 321–324, doi:10.1038/nphys1910.

Zhang, J. A., and W. M. Drennan, 2012: An observational study of vertical eddy diffusivity in the hurricane boundary layer. *J. Atmos. Sci.*, **69**, 3223–3236, doi:10.1175/JAS-D-11-0348.1.

——, and M. T. Montgomery, 2012: Observational estimates of the horizontal eddy diffusivity and mixing length in the low-level region of intense hurricanes. *J. Atmos. Sci.*, **69**, 1306–1316, doi:10.1175/JAS-D-11-0180.1.

——, P. G. Black, J. R. French, and W. M. Drennan, 2008: First direct measurements of enthalpy flux in the hurricane boundary layer: The CBLAST results. *Geophys. Res. Lett.*, **35**, L14813, doi:10.1029/2008GL034374.

——, F. D. Marks Jr., M. T. Montgomery, and S. Lorsolo, 2011: An estimation of turbulent characteristics in the low-level region of intense Hurricanes Allen (1980) and Hugo (1989). *Mon. Wea. Rev.*, **139**, 1447–1462, doi:10.1175/2010MWR3435.1.

Zhao, K., W. C. Lee, and B. J. D. Jou, 2008: Single Doppler radar observation of the concentric eyewall in Typhoon Saomai, 2006, near landfall. *Geophys. Res. Lett.*, **35**, L07807, doi:10.1029/2007GL032773.

Zhu, P., J. A. Zhang, and F. J. Masters, 2010: Wavelet analyses of turbulence in the hurricane surface layer during landfalls. *J. Atmos. Sci.*, **67**, 3793–3805, doi:10.1175/2010JAS3437.1.